Available online at www.sciencedirect.com
SCIENCE DIRECT®
Biochemical and Biophysical Research Communications 312 (2003) 1159–1164
BBRC
www.elsevier.com/locate/ybbrc

# The SARS-CoV S glycoprotein: expression and functional characterization

Xiaodong Xiao,[a] Samitabh Chakraborti,[a] Anthony S. Dimitrov,[a] Kosi Gramatikoff,[b] and Dimiter S. Dimitrov[a,*]

[a] *Laboratory of Experimental and Computational Biology, CCR, NCI-Frederick, NIH, Frederick, MD 21702-1201, USA*
[b] *Abgent, San Diego, CA 92121, USA*

Received 5 November 2003

**Abstract**

We have cloned, expressed, and characterized the full-length and various soluble fragments of the SARS-CoV (Tor2 isolate) S glycoprotein. Cells expressing S fused with receptor-expressing cells at neutral pH suggesting that the recombinant glycoprotein is functional, its membrane fusogenic activity does not require other viral proteins, and that low pH is not required for triggering membrane fusion; fusion was not observed at low receptor concentrations. S and its soluble ectodomain, $S_e$, were not cleaved to any significant degree. They ran at about 180–200 kDa in SDS gels suggesting post-translational modifications as predicted by previous computer analysis and observed for other coronaviruses. Fragments containing the N-terminal amino acid residues 17–537 and 272–537 but not 17–276 bound specifically to Vero E6 cells and purified soluble receptor, ACE2, recently identified by M. Farzan and co-workers [Nature 426 (2003) 450–454]. Together with data for inhibition of binding by antibodies developed against peptides from S, these findings suggest that the receptor-binding domain is located between amino acid residues 303 and 537. These results also confirm that ACE2 is a functional receptor for the SARS virus and may help in the elucidation of the mechanisms of SARS-CoV entry and in the development of vaccine immunogens and entry inhibitors.
Published by Elsevier Inc.

*Keywords:* SARS-CoV; S glycoprotein; Receptor; Binding; Fusion; Inhibitor; Vaccine

Viral envelope glycoproteins initiate entry of viruses into cells by binding to cell surface receptors followed by conformational changes leading to membrane fusion and delivery of the genome in the cytoplasm [1]. The spike (S) glycoproteins of coronaviruses are no exception and mediate binding to host cells followed by membrane fusion; they are major targets for neutralizing antibodies and form the characteristic corona of large, distinctive spikes in the viral envelopes [2,3]. Such 20- to 40-nm complex surface projections also surround the periphery of the SARS-CoV particles [4]. The level of overall sequence similarity between the predicted amino acid sequence of the SARS-CoV S glycoprotein and the S glycoproteins of other coronaviruses is low (20–27% pairwise amino acid identity) except for some conserved sequences in the S2 subunit [5]. The low level of sequence similarity precludes definite conclusions about functional and structural similarity. The SARS-CoV S glycoprotein has not been characterized biochemically and biophysically, and its receptor-binding domain (RBD) has not been localized. Here we report cloning, expression, and characterization of the SARS-CoV full-length S glycoprotein and various soluble fragments, demonstration of its fusogenic function at neutral pH, development of a quantitative cell fusion reporter gene-based assay, and localization of the RBD in the N-terminal 303–537 residues.

## Materials and methods

*Antibodies and plasmids.* New Zealand rabbits were immunized with 0.1 mg of various peptides selected by a computer program for their immunogenicity. Serum from the immunized rabbits was tested in

* Corresponding author. Fax: 1-301-846-6189.
*E-mail address:* dimitrov@ncifcrf.gov (D.S. Dimitrov).

0006-291X/$ - see front matter. Published by Elsevier Inc.
doi:10.1016/j.bbrc.2003.11.054

ELISA and Western blot for reactivity. Sera from rabbits immunized with two peptides exhibited the highest and specific activity against the S glycoprotein and were selected for this study. The antibodies denoted D24 and P540 were elicited by the peptides DVQAPNYTQH TSSMRGC and PSSKRFQPFQQFGRDC, respectively. Another anti-SARS-CoV S glycoprotein polyclonal antibody IMG-542, which recognizes amino acid 288–303 of the S glycoprotein, was purchased from IMGENEX (San Diego, CA). Plasmids encoding ACE2, pCDNA3-ACE2, and its soluble form, pCDNA3-ACE2-ecto, were kindly provided by M. Farzan from Harvard Medical School, Boston, MA. VTF7.3 and VCB21R are kind gifts from C. Broder, USUHS, Bethesda, MD. Expression vectors pCDNA3 and pSecTag2 series were purchased from Invitrogen (Carlsbad, CA).

*Construction of full-length S glycoprotein cDNAs and cloning in expression vectors.* Three pBR194c-based plasmids containing overlapping cDNAs that cover the full-length S glycoprotein coding sequence were purchased from the British Columbia Cancer Agency (BC, Canada). The following primers were used for amplification and overlapping PCR cloning of the full-length S glycoprotein: #1, 5′ AGTCGGATCC GGTAGGCTTATCATTAGAG 3′; #2, 5′ CCAT CAGGGGAGAA AGG CAC 3′; #3, 5′ GTGCCTTTCTCCCCTGATGG 3′; #4, 5′ GA AGAGCAGCGCCAGCACC 3′; #5, 5′ GGTGCT GGCGCTGCTC TTC 3′; and #6, 5′ ACTGTCTAGAGTTCGTTT ATGTGTAATG 3′. The amplified full-length S gene was cut with *Bam*HI and *Xba*I and ligated into the corresponding restriction sites in pCDNA3 plasmid to create pCDNA3-S. This plasmid was used to generate various soluble fragments of the S glycoprotein. The pair of primers #7, 5′ AGTCGGAT CCGACCGGTGCACCACTTTTG 3′ and #8, 5′ AGTCGGGCCCCT GTTCAGCAGCAATACC 3′ was used to amplify the S1 fragment containing residues 17–756. The fragment was cut with *Bam*HI and *Apa*I and cloned into corresponding sites of expression vector pSecTag2B (Invitrogen). Primer #7 and primer #9 5′ CTAGCTCGAGCAA-CAGCATCTGTG 3′ were used to amplify fragment S276 containing residues 17–276. The fragment was cut with *Bam*HI and *Xho*I and cloned into the corresponding sites in the pSecTag2B vector. Fragment S537 was generated by cutting S1 with *Bam*HI and *Hin*cII and cloned into pSecTag2B cut with *Bam*HI and *Eco*RV. To generate soluble S glycoprotein ectodomain, $S_e$, site-directed mutagenesis was performed to create an *Apa*I site upstream to the transmembrane domain of the S glycoprotein gene in pCDNA3-S. Then this plasmid was digested with *Pst*I and *Apa*I and the resulting fragment was used to replace the *Pst*I–*Apa*I fragments from pSecTag2B-S1, creating the pSecTag2B-$S_e$ plasmid. *Pst*I–*Apa*I fragment from pCDNA3-S was used to replace the *Pst*I–*Apa*I fragment from pSecTag2B-$S_e$ to create pSecTag2B-S without tags. To create the fragment containing residues 272–537, the following pair of primers, primer #10 5′ GATCGGATCCGGTACAATCACAG 3′ and primer #11 5′ GATCGGGCCCGACACACTGGTTC 3′, was used for PCR amplification. The amplified fragment was digested with *Bam*HI and *Apa*I and ligated to pSecTag2B digested with the same restriction enzymes. All S fragments and full-length S constructed in pSecTag2B had their native leader sequence (aa 1–16) replaced with a mouse k chain leader sequence.

*Protein expression.* Vero E6 or 293 cells were transfected with various plasmids using the Polyfect transfection kit from Qiagen (Valencia, CA) following the manufacturer's protocol. Four hours after transfection, cells were infected with VTF7.3 recombinant vaccinia virus encoding the gene for the T7 polymerase. The soluble fragments were obtained from the cell culture medium. The full-length S glycoprotein was detected only from cell lysate.

*Immunoprecipitation and purification.* Medium from cells transfected with various soluble S fragments was collected and subjected to centrifugation at 1000*g* for 10 min to remove cellular debris. The cleared medium was incubated with either Ni–NTA agarose beads (Qiagen, Valencia, CA) or immunoprecipitating antibody plus glycoprotein G–Sepharose beads (Sigma, St. louis, MO) for 2 h at 4 °C. The beads were then mixed with an equal volume of SDS gel sample buffer, boiled for 3 min, and subjected to gel analysis. For full-length S glycoprotein, cells were lysed first in PBS supplemented with 1% NP-40 and 0.5 mM PMSF for 1 h at 4 °C, and centrifuged at 14,000 rpm in a table-top Eppendorf centrifuge for 20 min. The cleared lysate was either immunoprecipitated first or used directly in Western blotting.

*Western blotting and slot blots.* Cells expressing the S glycoprotein were lysed first with a PBS-based NP40 lysis buffer as described above, and the debris were cleared by centrifugation. For soluble S fragments the medium was collected and cleared as described above. For slot blot, the cleared lysate or medium from supernatant was used directly to blot the nitrocellulose membrane following the protocol suggested by the manufacturer (Bio-Rad, Hercules, CA) and the membrane was subjected to antibody detection as in conventional Western blotting. For Western blotting, the monoclonal anti-c-Myc epitope antibody (Invitrogen, Carlsbad, CA) or the rabbit polyclonal antibodies obtained by immunization of rabbits with peptides were diluted in TBST buffer and incubated with the membrane for 2 h, washed and then incubated with the secondary antibody conjugated with HRP for 1 h, washed four times, each time for 15 min, and then developed using the ECL reagent (Pierce, Rockford, IL).

*Cell-binding assay and ELISA.* Medium containing soluble S fragments was collected and cleared by centrifugation. Vero E6 or other cells ($5 \times 10^6$) were incubated with 0.5 ml of cleared medium containing soluble S fragments and 2 μg of anti-c-Myc epitope antibody conjugated with HRP at 4 °C for 2 h. Cells were then washed three times with ice-cold PBS and collected by centrifugation. The cell pellets were incubated with ABTS substrate from Roche (Indianapolis, IN) at RT for 10 min, the substrate was cleared by centrifugation, and OD405 was measured.

For ELISA, purified ACE2 (R&D, Minneapolis, MN) was blocked to Maxisorp ELISA plate in pH 9.6 buffer at 100 ng per well. Medium (150 μl) containing various soluble S fragments and 0.6 μg of anti-c-Myc epitope antibody conjugated with HRP were incubated in each well at 37 °C for 2 h. Wells were washed and 60 μl of ABTS substrate was added to each well. OD405 was measured 20 min later.

*Fluorescent dye redistribution cell fusion assay.* HeLa or 293T cells, transfected with plasmids encoding the S glycoprotein, were loaded with Calcein AM (Molecular Probes), which is converted in cells to calcein green. The cells were incubated in medium containing 1 μg/ml Calcein AM for 1 h at 37 °C and 5% $CO_2$, and then washed and resuspended in fresh medium. Plated target cells, Vero E6, were stained with CMAC (Molecular Probes) by incubation in 1 μg/ml CMAC in medium for 30 min at 37 °C and 5% $CO_2$, then the cells were washed twice with medium and incubated for 20 min in fresh medium and washed again, and then covered with 0.5 ml medium in each well. The S-expressing cells, loaded with calcein, were added to the target cells and incubated for 1, 2, or 4 h at 37 °C and 5% $CO_2$. Fusion was measured as the ratio between the cells that have double staining and the total number of target cells in contact with an S glycoprotein-expressing cell. Microphotographs were taken by using MethaMorph 4.0 software from Universal Imaging.

*β-Galactosidase reporter gene-based cell–cell fusion assay.* 293T cells ($1.5 \times 10^6$) were plated in T25 flasks one day before transfection. The next day, these cells were transfected with pCDNA3-S, pSectag2B-S, pCDNA3-ACE2, and pCDNA3-ACE2-Ecto, respectively, using the Polyfect transfection kit (Qiagen, Valencia, CA) following the manufacturer's suggested protocol. Four hours after transfection, cells transfected with S constructs were infected with T7 polymerase-expressing vaccinia virus VTF7.3 and cells transfected with ACE-2 constructs were infected with β-gal encoding vaccinia virus (VCB21R). Two hours after infection, cells were incubated with fresh medium and transferred to 31 °C for overnight incubation. The next day S glycoprotein-expressing cells and ACE-2-expressing cells were mixed in 1:1 ratio and incubated at 37 °C. Three hours later, cells were lysed by adding NP-40 to a final concentration of 0.5%. Cell lysate (50 μl) was mixed with equal volume of CPRG substrate and OD595 was measured 1 h later.

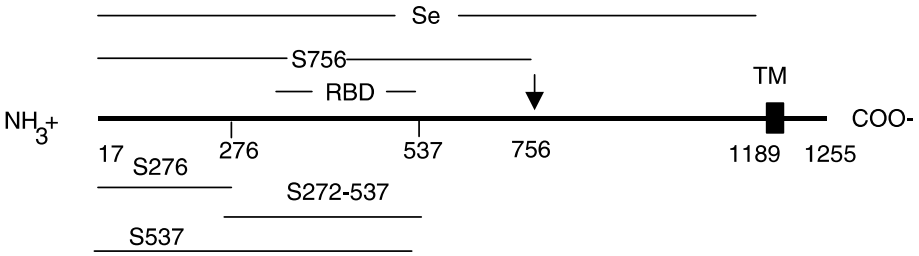


Fig. 1. Schematic diagram of a monomer of expressed full-length SARS-CoV S glycoprotein and various soluble fragments after removal of the signal sequence (residues 1–16). TM denotes the transmembrane segment and the arrow indicates possible cleavage site at amino acid residues 758–761 (RNTR). RBD indicates the potential receptor-binding domain that is within S272–537 likely between a residue downstream from 303 and a residue upstream of 537 as suggested by this work.

## Results and discussion

*Cloning, expression, purification, and general characterization of full-length S glycoprotein and soluble fragments*

To characterize the properties and function of the SARS-CoV S protein we cloned in expression vectors the DNAs encoding the full-length Tor2 isolate [6] S protein (1255 residues), the ectodomain $S_e$ (residues 17–1189) where the S putative transmembrane domain and cytoplasmic tail were deleted, fragments containing the N-terminal 276, 537, and 756 amino acid residues (S276, S537, and S756, respectively) including a putative 16-residue signal sequence [5] or a mouse k chain leader sequence, and an internal fragment (S272–537) containing residues 272–537 (Fig. 1). We noted that a stretch of amino acid residues (758–761, RNTR) is a particular case of the general motif K/R–$X_n$–K/R (X is any residue and $n = 0$, 2, 4 or 6) for cleavage by precursor convertases. Thus S756 approximates S1 in agreement with the size of S1 for murine coronaviruses, e.g., strain JHM where S1 is 769 residues [7] and

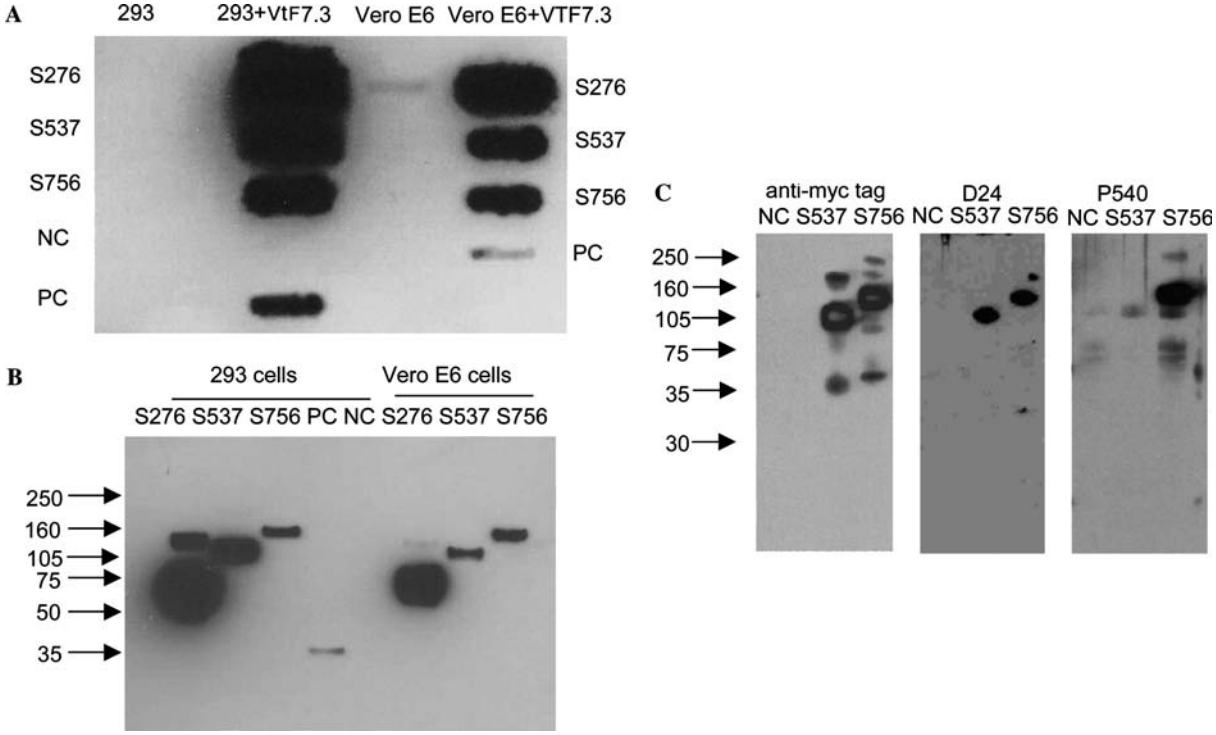


Fig. 2. Expression of soluble S fragments. (A) Supernatants of 293 and Vero E6 cells transfected with plasmids encoding S fragments (S276, S537, and S756) in the absence or presence of T7 polymerase expressed by recombinant vaccinia virus (VTF7.3) were transferred to nitrocellulose membranes (dot blots) and detected with anti-c-Myc epitope antibody. PC is the positive control for this antibody provided by the manufacturer and NC is a negative control of cells transfected with empty vector. (B) Supernatants from transfected cells as described above (A) were incubated with Ni–NTA agarose beads, washed, and subjected to Western blotting with the same anti-c-Myc epitope antibody as in A. (C) Detection of S fragments by two rabbit polyclonal antibodies raised against peptides corresponding to sequences starting at residues 24 (D24) and 540 (P540), respectively (right two panels). The left panel shows for comparison Western blot where S537 and S756 were detected by the anti-c-Myc epitope antibody.

human coronavirus OC43 (778 residues) [8]; however, for the human coronavirus 229E S1 is considered to consist of a shorter 547 residue fragment which corresponds to S537 [9]. All proteins except the full-length S glycoprotein were tagged with a c-Myc epitope and a histidine tag.

These proteins were expressed in 293 and Vero E6 cells after transfection with the corresponding plasmids followed by infection with vaccinia virus-expressing T7 polymerase. The tagged proteins were detected by using an anti-c-Myc monoclonal antibody (Fig. 2). It is striking that the T7 promoter was much more efficient for expression of the S glycoprotein than the CMV promoter, which under most circumstances is a strong promoter (2A). The S fragments were soluble and their concentration in the culture supernatants was inversely proportional to their size (Fig. 2).

To be able to detect unlabeled proteins, validate the data obtained by the anti-c-Myc antibody, and localize possible antigenic sites we developed rabbit polyclonal antibodies. Two of these antibodies, D24 and P540 raised against peptides starting at residues 24 and 540, respectively, recognized specifically tagged soluble fragments (Fig. 2C). As expected D24 recognized all fragments; P540 recognized S756, $S_e$, and S but not the smaller fragments (Fig. 2C and data not shown). P540 was very sensitive even at dilution 1:10,000 and was mostly used in this study unlike D24 which was relatively weak. The full-length S glycoprotein was expressed at the cell surface, although at low levels as measured by flow cytometry (Fig. 3).

All S glycoprotein fragments and the full-length S glycoprotein ran on a SDS–PAGE gel at positions significantly higher than their estimated molecular weights, indicating the possibility for post-translational modifications. S276 had an apparent molecular weight of about 75 kDa, S537—100–110 kDa, S756—130–140 kDa, and $S_e$ and S—about 200 kDa or higher (Figs. 2 and 4). The bands were broad when observed at low exposure (Fig. 4 and data not shown). These data indicate significant glycosylation as observed for S glycoproteins from other coronaviruses. Based on approximate estimations of molecular weight it appears that S2 is not as heavily glycosylated as S756. Notably, S276 is heavily glycosylated if one assumes that only glycosylation contributes to the increased molecular mass. Most of the SARS-CoV S glycoprotein was not cleaved, although we observed weak bands due to smaller proteins, one of which runs at the same position as S756, suggesting the possibility for inefficient cleavage (Fig. 4). We cannot rule out the possibility of random digestion by proteases. Further studies are needed to determine if the S glycoprotein cleavage is necessary for its function.

We have not observed measurable cytopathic effects in cells transfected with any of the constructs we developed (data not shown) indicating the possibility that

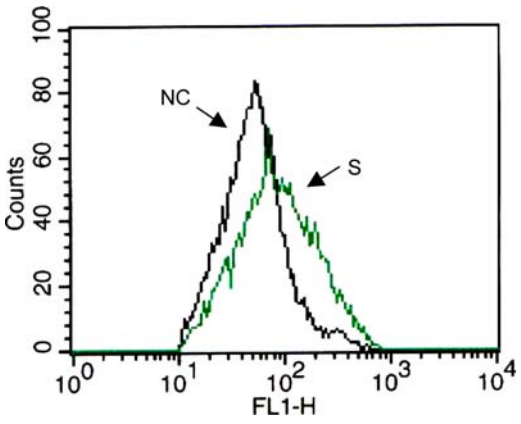


Fig. 3. Surface expression of full-length membrane-associated S protein demonstrated by flow cytometry using the rabbit polyclonal antibody P540. Full-length S glycoprotein was used to transfect 293 cells, which were then infected with VTF7.3. Cells were collected and incubated with P540 polyclonal antibody plus anti-rabbit secondary antibody conjugated with FITC, washed, and subjected to flow cytometry analysis. The same plasmid used to express S but without the gene for S was used to transfect cells in a control experiment denoted as negative control (NC); the full-length S glycoprotein is denoted as S.

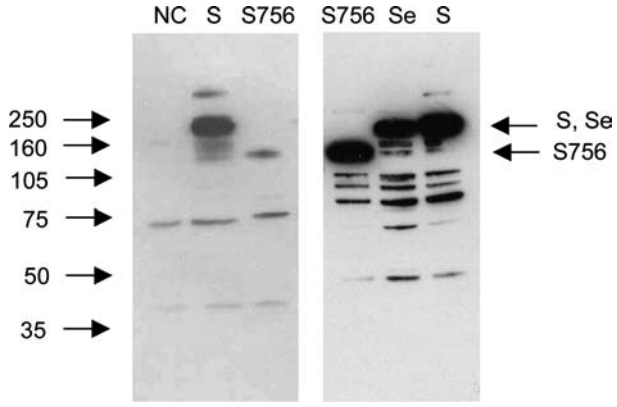


Fig. 4. Characterization of the S756, $S_e$, and S glycoproteins. Close to background level cleavage of S and $S_e$. Western blots of supernatants from transfected 293 cells expressing S756, $S_e$, and cell lysate of 293 cells expressing the S glycoproteins using the P540 antibody are shown. The left panel shows Western blots of samples kept for three days at 4 °C before analysis to monitor the effect of nonspecific protease activity on the cleavage pattern, whereas the right one—blots with samples used immediately after preparation.

the full-length and soluble fragments of the S glycoprotein may not have direct cytopathic effects. However, at higher levels of expression such effects are possible and obviously formation of syncytia as described in the next section could lead to cell death.

### *The full-length S glycoprotein mediates fusion at neutral pH with cells expressing receptor molecules*

To confirm that the full-length recombinant S glycoprotein is functional, and to find whether it requires

other viral proteins and low pH for its fusion activity, we performed cell–cell fusion assays. Expression of the full-length S glycoprotein with both vectors, pCDNA3-S and pSectag2B-S, supported fusion with ACE2 expressing cells efficiently, as evidenced by formation of syncytia of various sizes and a β-gal reporter gene-based assay (Fig. 5). Interestingly, the pSectag2B-S construct in which the S glycoprotein leader peptide was replaced by a mouse k chain leader sequence induced faster formation of syncytia that were larger and more numerous than those induced by pCDNA3-S, which encodes the native S glycoprotein (data not shown). The extent of fusion mediated by S expressed by using pSectag2B-S was also higher than by using pCDNA3-S as measured by a reporter gene-based assay (Fig. 5B). These data indicate that the S glycoprotein may not be efficiently transported to the cell surface but further studies are required to confirm this possibility. They also suggest that the β-gal assay described here can serve as a quick and quantitative method to identify inhibitors of the SAR-CoV entry into cells, as well as a tool to study SARS-CoV entry mechanism.

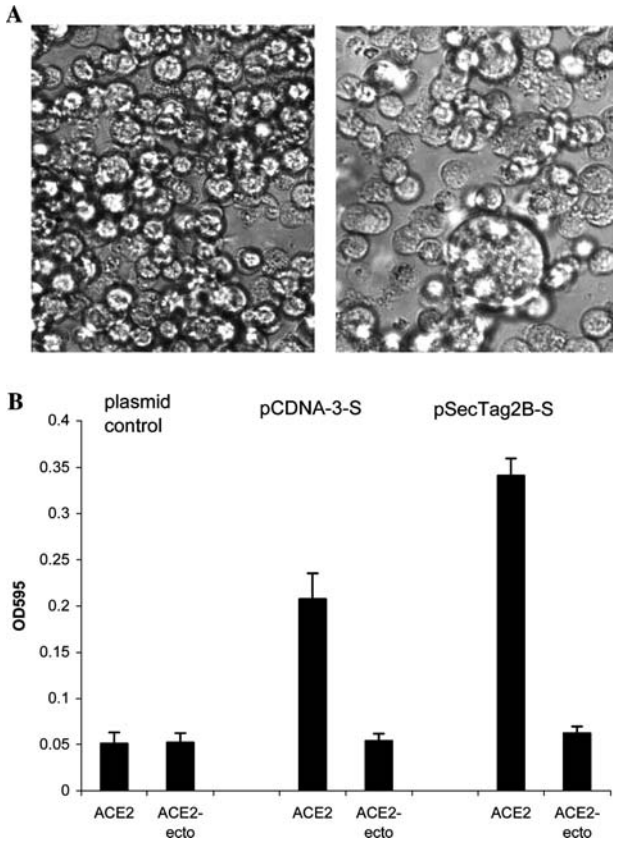


Fig. 5. Cell fusion mediated by the S glycoprotein. (A) Syncytium formation between 293T cells transfetced with pSecTag2B-S and pCDNA3-ACE2, respectively (right panel). There was no syncytium formation between 293T cells transfected with pSecTag2B-S and pCDNA3-ACE2-Ecto (left panel). (B) Cell fusion measured by a reporter gene-based assay. S glycoprotein expressed in both pCDNA3 and pSecTag2B vectors can be used in a β-gal reporter gene-based cell–cell fusion assay. A pCDNA3-based plasmid without S insert was used as plasmid control, and fusion between S-expressing cells with ACE2-ecto expressing cells was used as negative control.

Notably by using this assay and the syncytium formation assay we were not able to detect fusion of Vero E6 cells that were not transfected with plasmids encoding ACE2 and express only native concentrations of the receptor. To explore the possibility that this was due to low sensitivity of these two assays, we also used another assay based on fluorescent dye redistribution that is able to detect fusion of single cells. We were not able to detect statistically significant differences between cells transfected with plasmids encoding the full-length S glycoprotein and various negative controls including plasmids encoding soluble S fragments at different pH (data not shown), suggesting that the higher levels of receptor expression achieved by expression of recombinant ACE2 could be important for cell–cell fusion. The underlying mechanisms remain to be

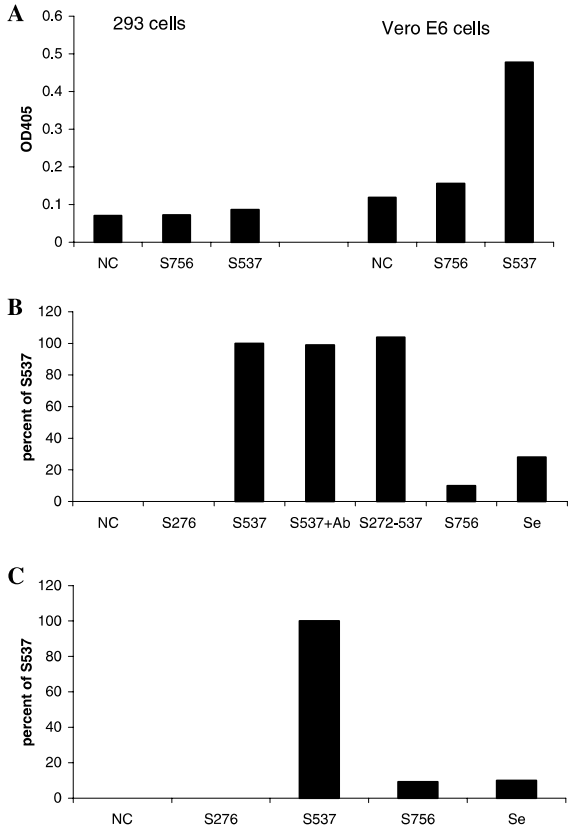


Fig. 6. Identification of the S glycoprotein receptor-binding domain (RBD). (A) Comparison of the binding of two different S soluble fragments (S537 and S756) to 293 and Vero E6 cells. (B) Binding of various S fragments to Vero E6 cells. The background OD405 measured for the negative control was subtracted from the OD405s of each S fragment. The resulting OD405 for each fragment was then presented as a percentage of the OD405 for S537. (C) Interaction of S fragments with purified soluble ACE2 as measured by ELISA. In all experiments, the negative control (NC) represents sample processed exactly the same way as the others except that the plasmid used for transfection did not encode any protein. Data shown here represent at least three independent experiments. OD405 for all samples is presented as percentages of that for S537.

elucidated and could play a role in the entry of cell-free virus into cells. It is also possible that higher levels of S expression could lead to measurable cell fusion, even when the receptor concentrations are relatively low. Overall, these results suggest that recombinant S glycoprotein alone can mediate cell fusion, that fusion can occur at neutral pH, and that its efficiency is dependent on the concentration of the receptor molecules.

*Identification of a receptor-binding domain*

In an attempt to localize the receptor-binding domain (RBD) of the S glycoprotein prior to the identification of the SARS-CoV receptor, we developed an assay based on the binding of various soluble fragments to receptor expressing Vero E6 cells. Incubation of Vero E6 cells that are susceptible to SARS-CoV infection and several cell lines that are not with soluble fragments resulted in binding only to Vero E6 cells by all fragments except the smallest one (S276) (Figs. 6A and B and data not shown). Binding was proportional to the expression levels of the fragments that were approximately inversely proportional to their sizes. These findings suggested that the RBD is localized between residues 272 and 537.

To further localize the RBD we used an antibody (IMG 542), which was elicited by a peptide containing residues 288–303. This antibody did not inhibit binding of the S537 fragment to Vero E6 cells although it did bind this fragment (Fig. 6B and data not shown), suggesting that the RBD is localized between residues 303 and 537. Because of the relatively large antibody size and the possibility for steric hindrance, one can assume that the RBD is even further downstream of residue 303. By contrast, the RBD for murine hepatitis virus was mapped to the N-terminal 330 amino acids (14). However, recently, the RBD of the HCoV-229E was localized to a fragment containing amino acid residues 407–547 (4,5). It remains to be seen whether there is structural similarity of these fragments with the RBD-containing fragments of the SARS-CoV S1 glycoprotein (e.g., S272–537), and whether such similarity is related to the use of the same host for replication, although these two viruses use different receptors. The straightforward cell-binding approach described here could also be helpful for identification of other virus receptors.

Very recently, Li et al. [10] reported the identification of ACE2 as a functional receptor for the SARS-CoV. The receptor identification allowed us to further validate our results by using purified ACE2. The same binding pattern was observed in ELISA as in the cell-binding assay with all tested S fragments (Fig. 6C). These results also confirm the receptor function of ACE2. Systematic studies are in progress to determine the critical residues involved in receptor binding. These findings not only offer new tools to study entry of the SARS virus into cells and localize the RBD but also could help in the development of novel vaccine immunogens and therapeutics for prevention and treatment of SARS.

## Acknowledgments

We thank C. Broder, K. Bossart, P. Bates, M. Farzan, K. Holmes, R. Blumenthal, and L. Anderson for helpful discussions. We appreciate the generous gift of plasmids encoding ACE2 from M. Farzan.

## References

[1] D.S. Dimitrov, Cell biology of virus entry, Cell 101 (2000) 697–702.
[2] K.V. Holmes, SARS-associated coronavirus, N. Engl. J. Med. 348 (2003) 1948–1951.
[3] M.M. Lai, D. Cavanagh, The molecular biology of coronaviruses, Adv. Virus Res. 48 (1997) 1–100.
[4] T.G. Ksiazek, D. Erdman, C.S. Goldsmith, S.R. Zaki, T. Peret, S. Emery, S. Tong, C. Urbani, J.A. Comer, W. Lim, P.E. Rollin, S.F. Dowell, A.E. Ling, C.D. Humphrey, W.J. Shieh, J. Guarner, C.D. Paddock, P. Rota, B. Fields, J. DeRisi, J.Y. Yang, N. Cox, J.M. Hughes, J.W. LeDuc, W.J. Bellini, L.J. Anderson, A novel coronavirus associated with severe acute respiratory syndrome, N. Engl. J. Med. 348 (2003) 1953–1966.
[5] P.A. Rota, M.S. Oberste, S.S. Monroe, W.A. Nix, R. Campagnoli, J.P. Icenogle, S. Penaranda, B. Bankamp, K. Maher, M.H. Chen, S. Tong, A. Tamin, L. Lowe, M. Frace, J.L. DeRisi, Q. Chen, D. Wang, D.D. Erdman, T.C. Peret, C. Burns, T.G. Ksiazek, P.E. Rollin, A. Sanchez, S. Liffick, B. Holloway, J. Limor, K. McCaustland, M. Olsen-Rasmussen, R. Fouchier, S. Gunther, A.D. Osterhaus, C. Drosten, M.A. Pallansch, L.J. Anderson, W.J. Bellini, Characterization of a novel coronavirus associated with severe acute respiratory syndrome, Science 300 (2003) 1394–1399.
[6] M.A. Marra, S.J. Jones, C.R. Astell, R.A. Holt, A. Brooks-Wilson, Y.S. Butterfield, J. Khattra, J.K. Asano, S.A. Barber, S.Y. Chan, A. Cloutier, S.M. Coughlin, D. Freeman, N. Girn, O.L. Griffith, S.R. Leach, M. Mayo, H. McDonald, S.B. Montgomery, P.K. Pandoh, A.S. Petrescu, A.G. Robertson, J.E. Schein, A. Siddiqui, D.E. Smailus, J.M. Stott, G.S. Yang, F. Plummer, A. Andonov, H. Artsob, N. Bastien, K. Bernard, T.F. Booth, D. Bowness, M. Czub, M. Drebot, L. Fernando, R. Flick, M. Garbutt, M. Gray, A. Grolla, S. Jones, H. Feldmann, A. Meyers, A. Kabani, Y. Li, S. Normand, U. Stroher, G.A. Tipples, S. Tyler, R. Vogrig, D. Ward, B. Watson, R.C. Brunham, M. Krajden, M. Petric, D.M. Skowronski, C. Upton, R.L. Roper, The genome sequence of the SARS-associated coronavirus, Science 300 (2003) 1399–1404.
[7] T.M. Gallagher, M.J. Buchmeier, Coronavirus spike proteins in viral entry and pathogenesis, Virology 279 (2001) 371–374.
[8] F. Kunkel, G. Herrler, Structural and functional analysis of the surface protein of human coronavirus OC43, Virology 195 (1993) 195–202.
[9] A. Bonavia, B.D. Zelus, D.E. Wentworth, P.J. Talbot, K.V. Holmes, Identification of a receptor-binding domain of the spike glycoprotein of human coronavirus HCoV-229E, J. Virol. 77 (2003) 2530–2538.
[10] W. Li, M.J. Moore, N. Vasilieva, J. Sui, S.K. Wong, M.A. Berne, M. Somasundaran, J.L. Sullivan, K. Luzuriaga, T.C. Greenough, H. Choe, M. Farzan, Angiotensin-converting enzyme 2 is a functional receptor for the SARS coronavirus, Nature 426 (2003) 450–454.